

ADA 020 552

RIA-76-U166

Attn: *W. W. Beyth*
AMSAR-ECT,
Mr. W. Beyth

ADA 02 055 2

USADACS Technical Library



5 0712 01004467 4

FA-TR-75034

ELECTRICAL PROPERTIES OF As_2S_3 GLASS

TECHNICAL
LIBRARY

March 1975

Approved for public release; distribution unlimited.



PITMAN-DUNN LABORATORY

U.S. ARMY ARMAMENT COMMAND
FRANKFORD ARSENAL
PHILADELPHIA, PENNSYLVANIA 19137

DISPOSITION INSTRUCTIONS

Destroy this report when it is no longer needed. Do not return it to the originator.

The findings in this report are not to be construed as an official Department of the Army position unless so designated by other authorized documents.

-- 1 OF 1
-- 1 - AD NUMBER: A020552
-- 2 - FIELDS AND GROUPS: 20/12
-- 3 - ENTRY CLASSIFICATION: UNCLASSIFIED
-- 5 - CORPORATE AUTHOR: FRANKFORD ARSENAL PHILADELPHIA PA
-- 6 - UNCLASSIFIED TITLE: ELECTRICAL PROPERTIES OF AS2S3 GLASS.
-- 8 - TITLE CLASSIFICATION: UNCLASSIFIED
-- 9 - DESCRIPTIVE NOTE: TECHNICAL RESEARCH REPT.,
--10 - PERSONAL AUTHORS: BOBB,LLOYD C. ;BYER,HAROLD H. ;KRAMER,KIMBALL ;
--11 - REPORT DATE: MAR , 1975
--12 - PAGINATION: 35P MEDIA COST: \$ 6.00 PRICE CODE: AA
--14 - REPORT NUMBER: FA-TR-75034
--16 - PROJECT NUMBER: DA-1-T-161102-A-31-C
--20 - REPORT CLASSIFICATION: UNCLASSIFIED
--23 - DESCRIPTORS: *PYROELECTRICITY, ARSENIC COMPOUNDS, SULFIDES,
-- OPTICAL GLASS, DIELECTRIC PROPERTIES, ALUMINUM, BAND THEORY OF
-- SOLIDS, ENERGY BANDS, ELECTRICAL PROPERTIES, OPTICAL PROPERTIES
--24 - DESCRIPTOR CLASSIFICATION: UNCLASSIFIED
--25 - IDENTIFIERS: *ARSENIC SULFIDES
--26 - IDENTIFIER CLASSIFICATION: UNCLASSIFIED
--27 - ABSTRACT: ALUMINIZED PLATELETS OF AS2S3 GLASS WERE POLED AT
-- TEMPERATURES AS HIGH AS 220C AND WITH ELECTRIC FIELDS UP TO 16 KV/
-- <<P FOR NEXT PAGE>> OR <<ENTER NEXT COMMAND>>

MSG RECEIVED

1a ROW=24 COL= 01

<Ctrl>H For Help

N Poll

UNCLASSIFIED

SECURITY CLASSIFICATION OF THIS PAGE (When Data Entered)

REPORT DOCUMENTATION PAGE		READ INSTRUCTIONS BEFORE COMPLETING FORM
1. REPORT NUMBER FA-TR-75034	2. GOVT ACCESSION NO.	3. RECIPIENT'S CATALOG NUMBER
4. TITLE (and Subtitle) ELECTRICAL PROPERTIES OF As ₂ S ₃ GLASS		5. TYPE OF REPORT & PERIOD COVERED Technical Research Report
7. AUTHOR(s) LLOYD C. BOBB HAROLD H. BYER KIMBALL KRAMER		6. PERFORMING ORG. REPORT NUMBER
9. PERFORMING ORGANIZATION NAME AND ADDRESS FRANKFORD ARSENAL ATTN: PDS-A PHILADELPHIA, PA 19137		8. CONTRACT OR GRANT NUMBER(s)
11. CONTROLLING OFFICE NAME AND ADDRESS USA ECOM FT. MONMOUTH NJ 07703		10. PROGRAM ELEMENT, PROJECT, TASK AREA & WORK UNIT NUMBERS AMCMS CODE: 691100.11.84500.01 DA PROJECT: 1T161102A31C
14. MONITORING AGENCY NAME & ADDRESS (if different from Controlling Office)		12. REPORT DATE March 1975
		13. NUMBER OF PAGES 36
		15. SECURITY CLASS. (of this report) UNCLASSIFIED
16. DISTRIBUTION STATEMENT (of this Report) Approved for public release; distribution unlimited.		15a. DECLASSIFICATION/OOWNGRADING SCHEDULE N/A
17. DISTRIBUTION STATEMENT (of the abstract entered in Block 20, if different from Report)		
18. SUPPLEMENTARY NOTES		
19. KEY WORDS (Continue on reverse side if necessary and identify by block number) As ₂ S ₃ Glass Dielectric Constant Resistivity Band Gap Pyroelectricity Polarization Charge Trapped Charge		
20. ABSTRACT (Continue on reverse side if necessary and identify by block number) Aluminized platelets of As ₂ S ₃ glass were poled at temperatures as high as 220°C and with electric fields up to 16 kV/cm. Electrical measurements on these samples yield the following results: (a) aluminum forms an ohmic contact with the glass, (b) the resistivity [ρ] $\sim 10^{11}$ ohm-cm, (c) the dielectric constant [ϵ] ~ 11 , (d) the electrical band gap is 2.40 eV as compared to 2.40 eV for the optical band gap, (e) the depolarization current generated by the samples is not of pyroelectric origin, (f) the polarization charge on the sample is as		

DD FORM 1473
1 JAN 73

EDITION OF 1 NOV 65 IS OBSOLETE

UNCLASSIFIED

SECURITY CLASSIFICATION OF THIS PAGE (When Data Entered)

20. ABSTRACT (Continued)

high as 4μ coulombs/cm², (g) the depolarization current is described by more than one relaxation time, (h) the data fit a trapped charge model better than a dipolar model, (i) the trap levels measured in these experiments are in the range 1.0 to 1.4 eV, and (j) on the basis of these experiments there is no evidence of pyroelectricity in these samples.

TABLE OF CONTENTS

	<u>Page</u>
INTRODUCTION	3
PYROELECTRIC MATERIALS	3
EXPERIMENTAL PROCEDURE	4
I-V CHARACTERISTICS.	4
ACTIVATION ENERGY AND BAND GAP	7
POLING RESULTS	9
DIPOLAR MODEL RESULTS.	16
CHARGE TRAPPING.	22
CONCLUSIONS.	28
REFERENCES	31
DISTRIBUTION	32

List of Tables

TABLE

1. The relaxation times for the open circuit current and short circuit current discharge curves are shown at four temperatures. The integrated charge and peak current are also given. 13
2. The relaxation times for the open circuit and short circuit polarization versus time curves are shown at four temperatures. 19
3. The thermal relaxation times are shown for values of $E_c - E_t$ at temperatures of 160°C and 220°C 29

List of Illustrations

FIGURE

1. Poling Circuit: The sample is held in place and the voltage is applied via the sample holder. The current and the temperature are monitored continuously. 5
2. The linear I-V characteristic for As_2S_3 glass at 220°C is shown for fields up to 16 kV/cm. 6

List of Illustrations (Cont'd)

<u>FIGURE</u>	<u>PAGE</u>
3. A plot of the logarithm of the current versus 1/temperature for As_2S_3 glass and 12 kV/cm applied is shown.	8
4. The current variation with time and temperature is shown for poled As_2S_3 glass with no electric field applied	10
5. Short circuit current versus time curves are shown for poled As_2S_3 glass. The sample was poled and depoled at the temperatures indicated on the curves.	12
6. A series of current versus time measurements are shown for an As_2S_3 glass sample poled at $220^{\circ}C$ with 400 volts. The delay time between the termination of the poling voltage and the commencement of the short circuit discharge can be read from the graph.	14
7. Open circuit current versus time curves are shown for poled As_2S_3 glass. The sample was poled and depoled at the temperatures indicated on the curves.	15
8. The open circuit polarization versus time curves are shown for As_2S_3 glass after having been poled at the temperatures indicated.	17
9. The short circuit polarization versus time curves are shown for As_2S_3 glass after having been poled at the temperatures indicated.	18
10. The polarization of As_2S_3 glass is shown as a function of time for various poling voltages at a temperature of $160^{\circ}C$. .	20
11. The polarization of As_2S_3 glass is shown as a function of time for various poling voltages at a temperature of $180^{\circ}C$. .	23
12. The polarization of As_2S_3 glass is shown as a function of time for various poling voltages at a temperature of $200^{\circ}C$. .	24
13. The polarization of As_2S_3 glass is shown as a function of time for various poling voltages at a temperature of $220^{\circ}C$. .	25
14. Saturation polarization values are plotted as a function of 1/temperature for As_2S_3 glass.	26

INTRODUCTION

There is currently a need for large area, inexpensive pyroelectric detectors with a high depoling temperature and a large pyroelectric coefficient. This study was undertaken to look for pyroelectricity in poled chalcogenide glasses. As_2S_3 glass is composed of polar pyramidal As_2S_3 molecular groups which are weakly bonded to each other. If these molecular groups could be oriented through the application of an electric field at elevated temperatures and then frozen into the new position by lowering the temperature the glass would then be in a polar state. And, if the polarization associated with this polar state were temperature dependent, the material would then be pyroelectric.

The electrical and optical properties of the As-S system have been reported by various authors.^{1,2} Recent optical and Raman measurements,^{3,4} support the molecular model for As_2S_3 .⁵ The physical properties of the As-Se-Te system, which is similar to the As-S system, have been reviewed.⁶ The interest in amorphous chalcogenides arises primarily because of the applications to xerography and computer memories. Also, these materials have the ancillary benefits of being easily prepared, non-crystalline, electronic semiconductors, which are relatively insensitive to impurities.

PYROELECTRIC MATERIALS

Of the 32 point groups 10 have a unique polar axis and are therefore called polar crystals. The magnitude of the spontaneous polarization in these materials depends on temperature. If the temperature changes, charges appear on the crystal faces which are perpendicular to the polar axis. This is called the pyroelectric effect. If the crystal faces are electrically connected, a current will flow when the crystal temperature is changed. The current obeys the relationship:

$$I = AP(T) \frac{dT}{dt} \quad (1)$$

¹ R.L. Myuller and Z.U. Borisova, "Solid State Chemistry", Consultant Bureau, New York, pp. 168-179 (1966).

² F. Kosek and J. Tauc, Czech. J. Phys. **B 20**, 94 (197).

³ G. Lucovsky, Phys. Rev. **B 6**, #4, 1480 (1972).

⁴ R.J. Kobliska and S.A. Solin, Phys. Rev. **B 8**, #2, 756 (1973).

⁵ G. Lucovsky and R.M. Martin, J. Non-Cryst. Solids **8**, 185 (1972).

⁶ D.D. Thornburg, J. Elec. Mat'l's **2**, #4, 495 (1973).

where A is the crystal area, $P(T)$ is the pyroelectric coefficient and dT/dt is the time rate of change of the temperature. The pyroelectric coefficients in ($nC/cm^2 \text{ } ^\circ C$) for several well-known materials are as follows: $Sr_{.73}Ba_{.27}Nb_2O_6$ (280), $LiTaO_3$ (18), TGS (16-35), $LiNbO_3$ (8.3), and PVF_2 (2.4).

EXPERIMENTAL PROCEDURE

Bulk samples of As_2S_3 from Americal Optical Company were cut and polished into $1 \text{ cm} \times 1 \text{ cm} \times .025 \text{ cm}$ platelets; samples of the same size were also obtained from Servo Corporation. Some measurements were made on samples that were less than 1 cm^2 . The samples were subsequently aluminized or silvered on both sides. However, the silvered samples could not be used for electrical measurements because the silver readily diffuses into the As_2S_3 glass lowering the resistivity. The capacitance and D-value of each sample at 1 kHz were measured before and after the poling process on the General Radio Model 1683 RLC bridge. The results of these measurements are:

- (a) $\epsilon \sim 11$
- (b) $\rho \sim 10^{11} \text{ ohm-cm}$
- (c) ρ decreases slightly ($\sim 20\%$) after poling
- (d) aluminum does not readily diffuse into As_2S_3
- (e) silver readily diffuses into As_2S_3 substantially lowering the resistivity

The poling circuit shown in Figure 1 consists of a D.C. power supply in series with a 10^5 ohm limiting resistor, a 10^3 ohm voltage dividing resistor and the sample. The sample holder leads are made from thin walled stainless steel tubing to minimize thermal losses from the furnace. The aluminum sample block is much more massive than the As_2S_3 platelets in order to minimize temperature fluctuations. A chromel-alumel thermocouple is used to monitor the temperature of the aluminum block. The thermocouple output is electrically connected to one channel of a dual-pen strip chart recorder. This experimental arrangement allows the simultaneous monitoring of sample current and temperature as a function of time.

I-V CHARACTERISTICS

A plot of current vs. voltage for a sample temperature of $220^\circ C$ is shown in Figure 2. The I-V curve is the same for both current directions. It can be seen from this plot that the I-V characteristic is linear for voltages up to 400V (16 kV/cm). This linear I-V characteristic is taken as an indication of ohmic contacts. Some care must be taken in interpreting

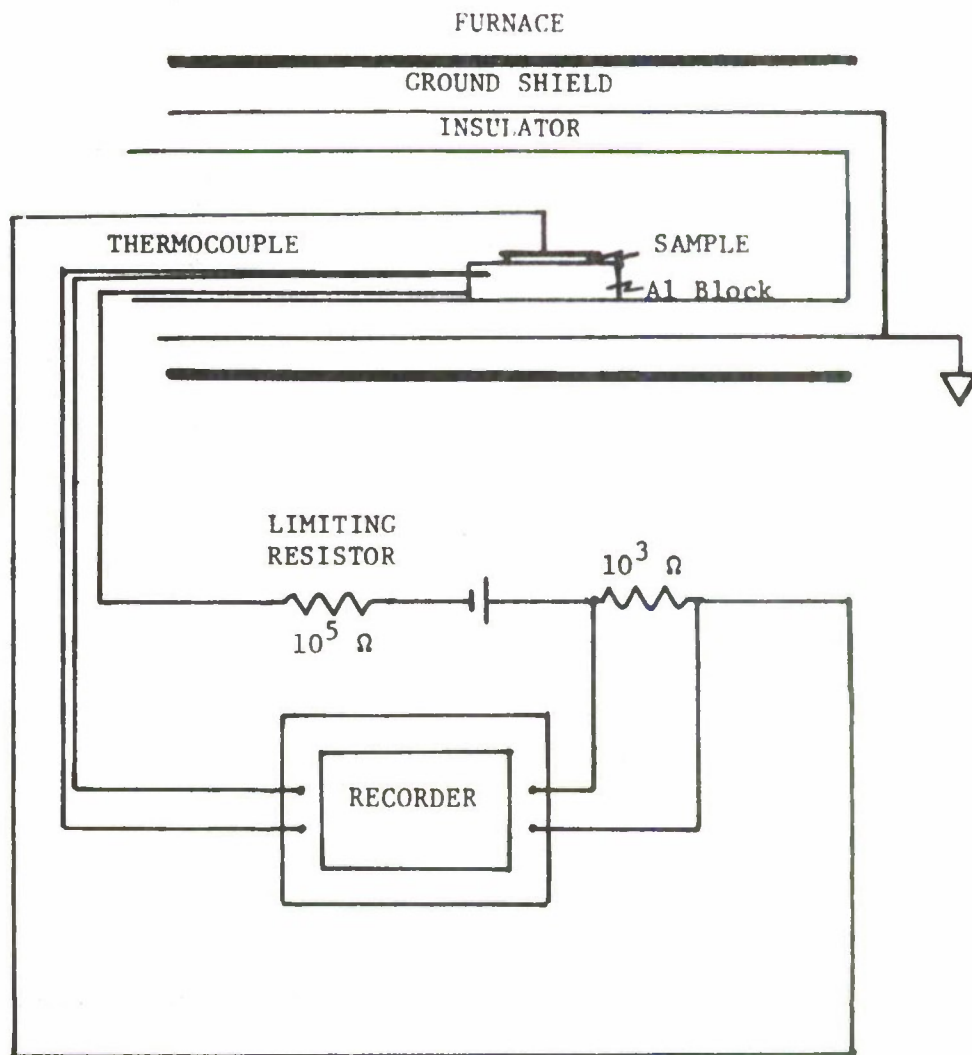


Figure 1. Poling Circuit: The sample is held in place and the voltage is applied via the sample holder. The current and the temperature are monitored continuously.

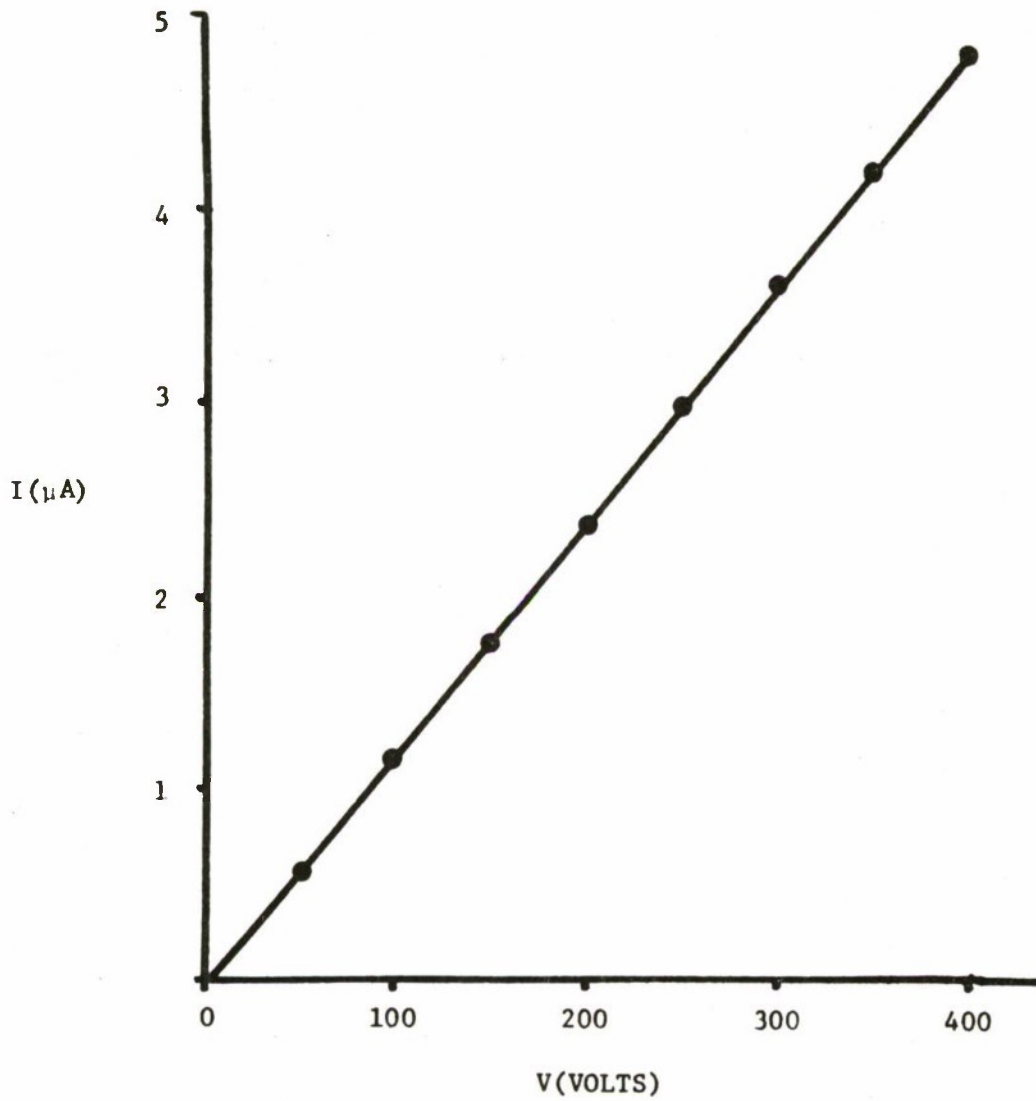


Figure 2. The linear I-V characteristic for As_2S_3 glass at 220°C shown for fields up to 16 kV/cm.

I-V characteristics in low mobility semiconductors. For example, with ohmic contacts the low current I-V characteristics is linear up to the point where more charge is injected than can be stored in the sample. At this point the current becomes space charge limited (SCL), that is, the carrier transit time equals the dielectric relaxation time. In this region (SCL) the I-V characteristic is not linear even though the contacts are perfectly injecting. At higher current densities the I-V curve can become electrode limited; that is, the effect of the electrode not supplying enough carriers will manifest itself in the I-V characteristics. The I-V characteristic can be linear in the electrode limited region. Therefore, a variety of I-V characteristics can arise with ohmic contacts.

ACTIVATION ENERGY AND BAND GAP

A log current vs. $1/\text{temperature}$ plot for As_2S_3 glass with aluminum electrodes and 300 V (12 kV/cm) applied is shown in Figure 3. The data can be fit by two straight lines intersecting near the softening temperature. If the current-temperature function is approximated in the following form.

$$I = I_0 \exp(-\phi/kT) \quad (2)$$

the activation energy (ϕ) is equal to 1.20 eV below the softening point and 1.53 eV above.

Kolomiets et al., determined the band gap of As_2S_3 by optical absorption measurements to be 2.40 eV at room temperature.⁷ The relationship between the activation energy and the band gap is described in Kittel⁸ for an intrinsic semiconductor as follows:

$$\phi = E_g/2 + 3/4 kT \log (m_h/m_e) \quad (3)$$

where m_h and m_e are the hole and electron masses respectively. If $m_h = m_e$, then the activation energy $\phi = E_g/2$. In amorphous semiconductors the Fermi level does not occur precisely in the middle of the forbidden band due to differences in the smearing of the valence and conduction bands. Therefore, the activation energy measured by the conduction process (1.20 eV) should be approximately one-half of the optical band gap (2.40 eV). The agreement here is good.

7

B.T. Kolomiets, T.F. Mazets, Sh. M. Efendieve, and A.M. Andriesh, J. Non-Cryst. Solids 4, 45 (1970).

8

C. Kittel, "Introduction to Solid State Physics", 3rd Edition, John Wiley & Sons, Inc., Inc., New York, p. 307.

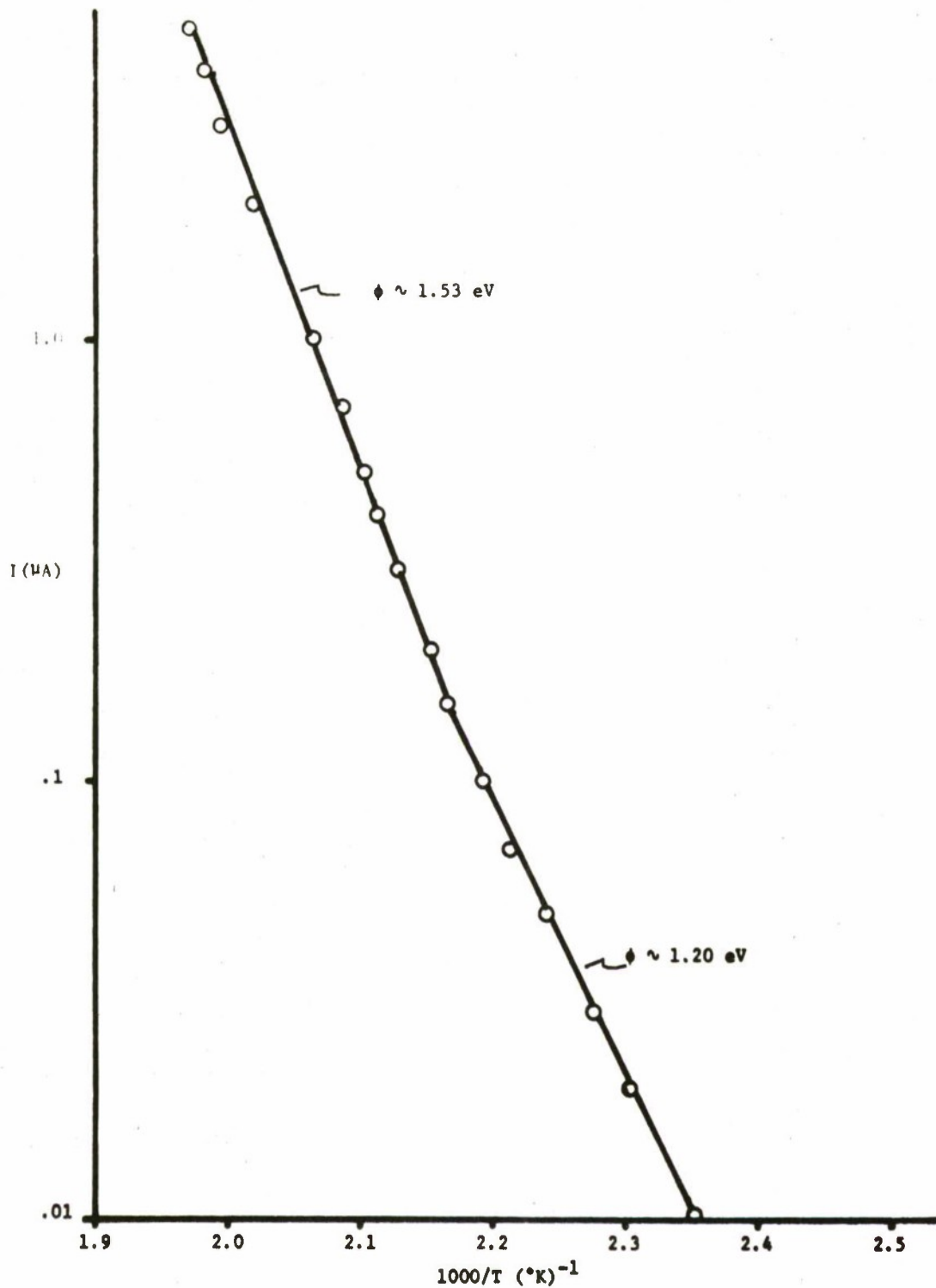


Figure 3. A plot of the logarithm of the current versus $1/\text{temperature}$ for As_2S_3 glass and 12 kV/cm applied is shown.

POLING RESULTS

Poling was attempted by applying electric fields up to 16 kV/cm while temperature cycling the samples from room temperature to 220°C and back to room temperature. The poled samples (without applied voltage) were then connected in series with a Keithley 150AR microvolt-ammeter. The temperature was then raised from 23°C to 220°C. The current generated by the sample and the temperature were monitored continuously; a typical plot is shown in Figure 4. It can be seen in Figure 4 that no measurable current is generated by the sample at temperatures below 125°C. At temperatures near 160°C the current rises sharply with temperature. The peak of this curve depends upon the poling history, the time-temperature history, and the magnitude of the temperature. The direction of current flow is in the same direction as when the sample is replaced by a capacitor. From integrating the current over the time and assuming that all of the charge is on the surface it is found that the surface charge density is as high as 4μ coulombs/cm². This corresponds to one electronic charge per 400 Å². For the purpose of comparison, BaTiO₃, a well-known ferroelectric material, has a remnant polarization of 25μ coulombs/cm². The charge/cm² stored in these samples due to the one kilohertz capacitance and the applied voltage is $15 \times 10^{-3}\mu$ coulombs/cm²; this is approximately 270 times smaller than the poling charge. If one considers that the charge is distributed throughout the volume of the material, the charge within the sample corresponds to 10^{15} charges/cm³. It is not unusual to have impurity concentrations in semiconductors of 10^{18} /cm³.

Equation 1 describes the current generated by a pyroelectric detector. The current from the samples (as in Figure 4) is not pyroelectric in origin because I is not zero when $dT/dt = 0$, I does not change sign with dT/dt and I is time dependent. If there is a pyroelectric current it is in the noise. For this experimental sensitivity this means that $P(T) \leq .36 \times 10^{-9}$ coulombs/cm² °C.

The maximum possible pyroelectric constant was estimated using a more sensitive apparatus. A poled specimen at room temperature was plunged into hot oil (80°C) and then into cold insulating oil (ca. 15°C). The specimen temperature was monitored with a thermistor embedded in a teflon specimen holder; the current from the specimen was monitored on a Keithley Electrometer, Model 616. Heating and cooling rates as high as 15°C/min were achieved. The electrometer and thermistor outputs were fed through a digital data acquisition system into a Wang calculator where the pyroelectric constant and temperature change were calculated and tabulated; and the pyroelectric constant versus temperature was plotted. From this data we estimate that the pyroelectric constant must be less than 1×10^{-12} coulombs/cm² °C. It is possible for the samples to be polar and to have a negligible pyroelectric coefficient if the dipole moment is temperature insensitive.

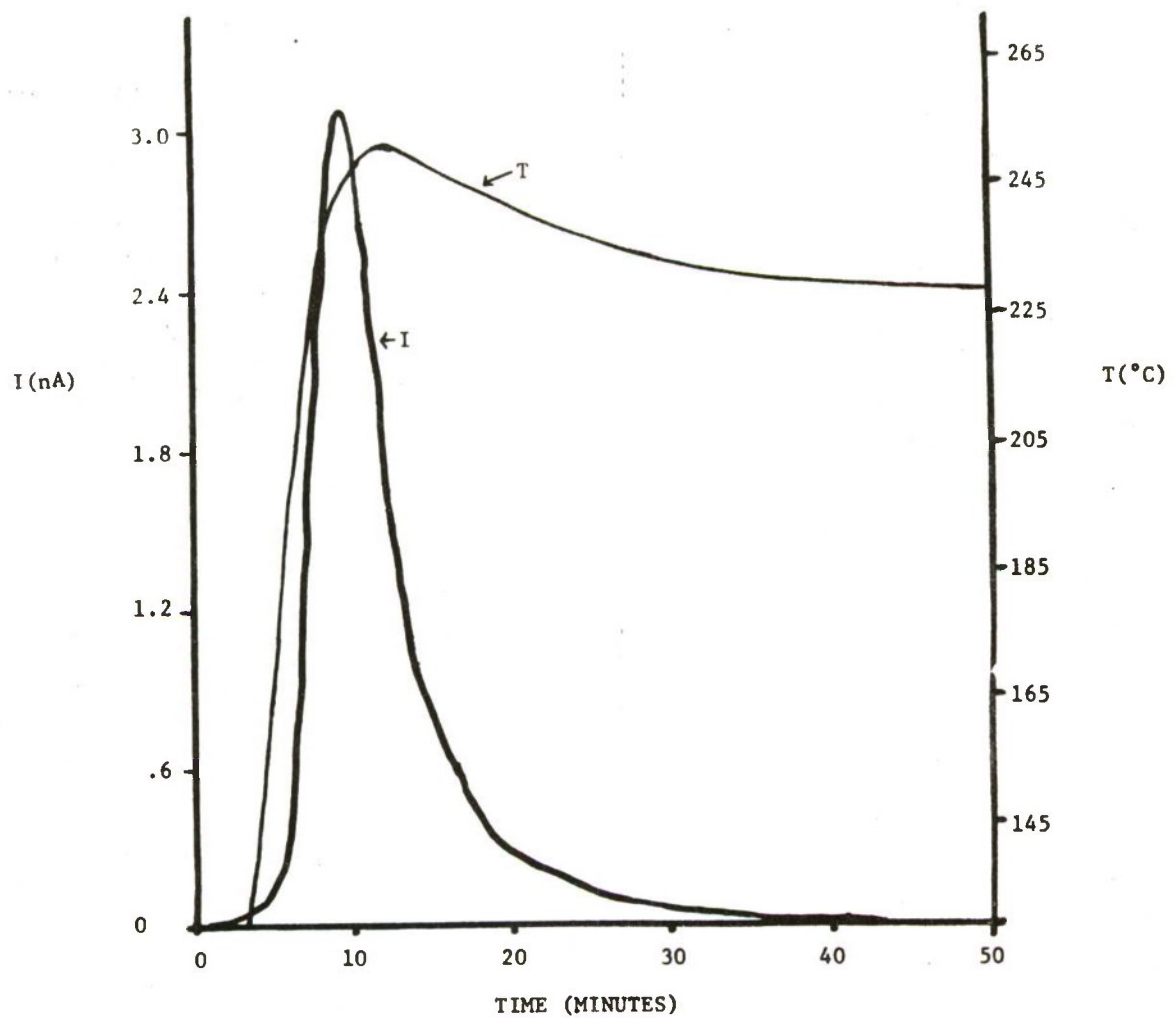


Figure 4. The current variation with time and temperature is shown for poled As_2S_3 glass with no electric field applied.

An explanation for the observed current in Figure 4 is that charge is trapped within the sample during the poling process and is subsequently released when the sample is heated. An alternate explanation is that the AsS_3 dipolar pyramids are partially aligned via the electric field and frozen into position when the sample is cooled. When the sample temperature is elevated the dipoles become disordered and a current flows to accommodate the change in polarization.

The current vs. time relationship was measured at $220^{\circ}C$, $200^{\circ}C$, $180^{\circ}C$, and $160^{\circ}C$ for various poling voltages in an effort to understand the polarization mechanism. In Figure 5 the current vs. time curves are shown for an As_2S_3 glass sample poled and depoled at the temperatures shown. These discharge curves were measured by short-circuiting the sample through the nanoammeter immediately after poling at 400 V (16 kV/cm) for 1 minute. It is evident from the curves that there is more than one relaxation time involved at each temperature. The relaxation times vary from about 10 seconds to 400 seconds. It is also evident in Figure 5 that the total charge varies considerably with temperature (~ 2300 nC at $220^{\circ}C$ and ~ 60 nC at $160^{\circ}C$). The short circuit current relaxation times ($[\tau_{I,SC}^{(slow)}, \tau_{I,SC}^{(fast)}]$) at the four temperatures are shown in Table 1. The fast and slow relaxation times are taken at the beginning and end of each curve respectively. The open circuit current relaxation times ($[\tau_{I,OC}^{(slow)}, \tau_{I,OC}^{(fast)}]$) are also shown in Table 1. These values are obtained from the open circuit discharge curves which are measured by inserting various delay times between termination of the poling voltage and the commencement of the short circuit measurement. A typical example of a series of these measurements is shown in Figure 6. These are current vs. time curves where the delay time can be read directly from the graph. The open circuit discharge curves are shown in Figure 7. As can be seen from the curves and in Table 1, the relaxation times vary markedly.

On comparing the discharge curves in Figures 7 and 5, no simple relationship is found between the open circuit and short circuit curves. The major difference arises between the $220^{\circ}C$ curves where the open circuit values are much higher than the short circuit values. This same general behavior is seen also at $200^{\circ}C$; however, the differences are not as pronounced. At $180^{\circ}C$ the open circuit values fall below the short circuit values then level off to be higher. This same behavior is seen also at $190^{\circ}C$. At $160^{\circ}C$ the curves are quite similar over the limited range of values. In an attempt to analyze these results an equivalent circuit model of the electroded sample was used. It was assumed that the bulk of the sample could be represented by a capacitor in parallel with a resistance which decreases exponentially with temperature. The contact resistance is assumed to be temperature independent and in series with the capacitor. With this model the open circuit discharge curves arise from the capacitor discharging through the resistance with a time constant (RC) which depends on temperature. From the capacitance and resistance values for the samples

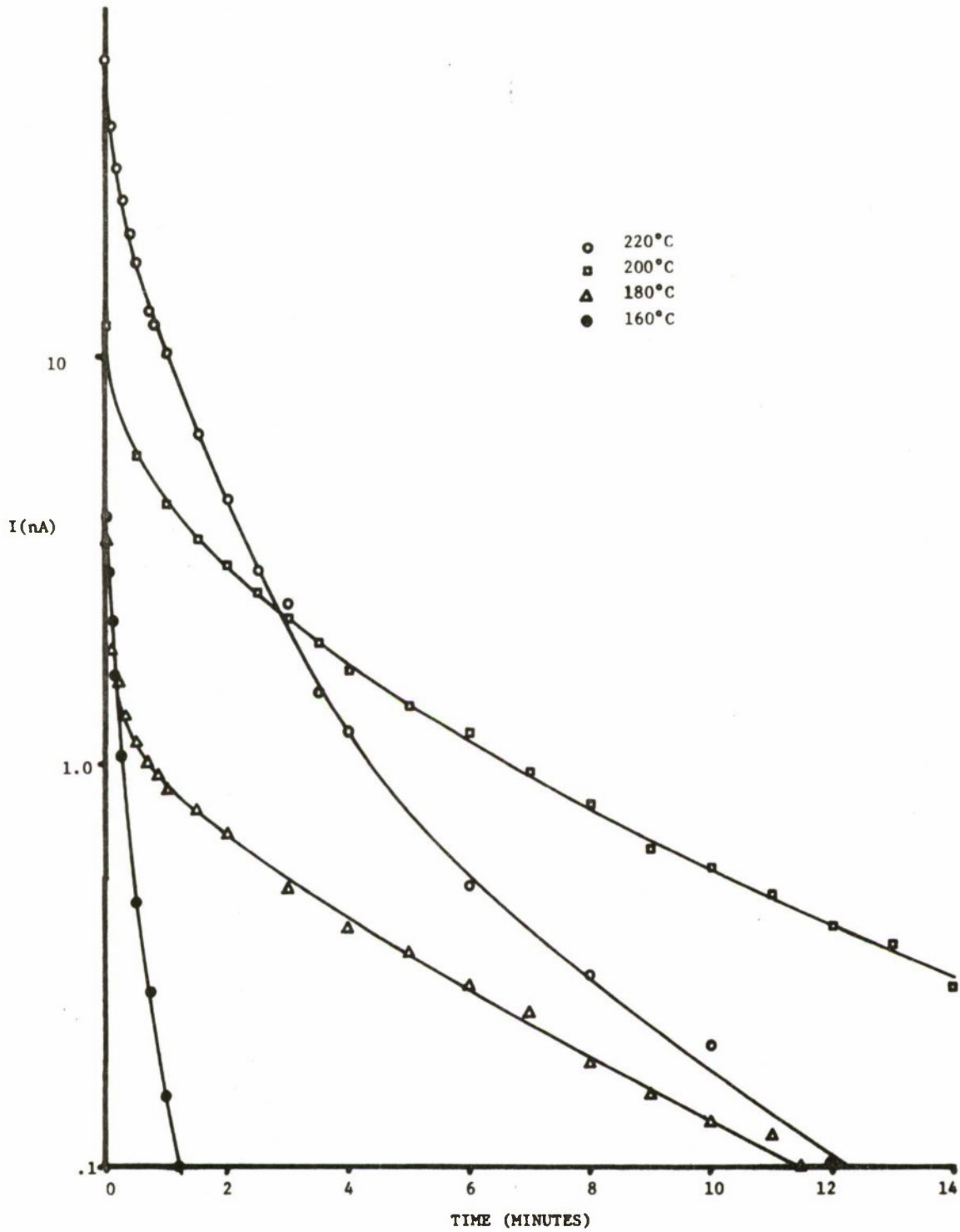


Figure 5. Short circuit current versus time curves are shown for poled As_2S_3 glass. The sample was poled and depoled at the temperatures indicated on the curves.

Table 1. The relaxation times for the open circuit current and short circuit current discharge curves are shown at four temperatures. The integrated charge and peak current are also given.

TEMPERATURE (°C)	$\tau_{I,SC}$ (slow) (seconds)	$\tau_{I,SC}$ (fast) (seconds)	$\tau_{I,OC}$ (slow) (seconds)	$\tau_{I,OC}$ (fast) (seconds)	INTEGRATED CHARGE (nanocoulombs)	PEAK CURRENT (nanoamperes)
160	97	9	49	13	60	4.1
180	390	12	4300	13	290	3.8
200	380	23	1250	25	1400	12
220	174	17	3120	25	2000	55

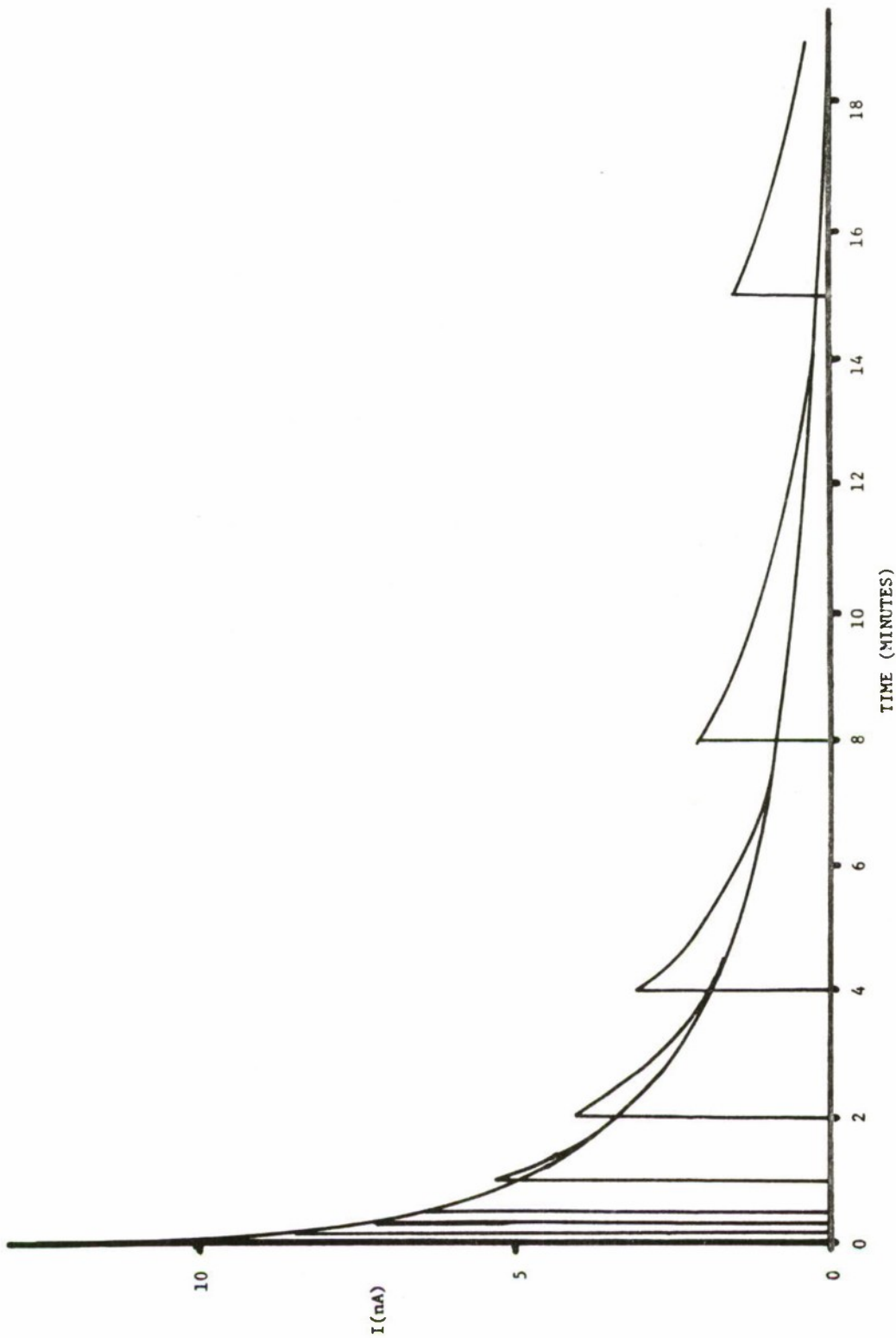


Figure 6. A series of current versus time measurements are shown for an As_2S_3 glass sample poled at 220°C with 400 volts. The delay time between the termination of the poling voltage and the commencement of the short circuit discharge can be read from the graph.

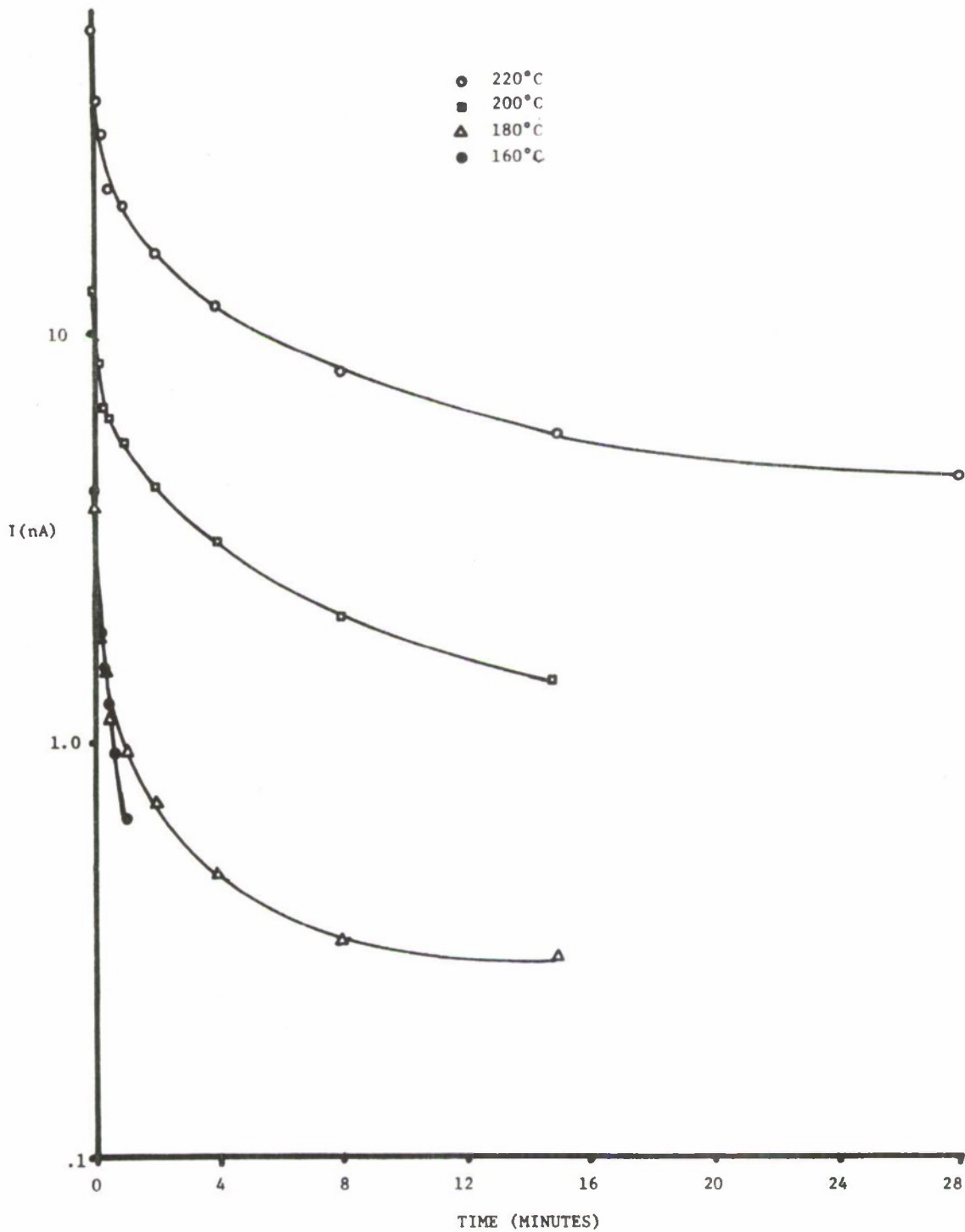


Figure 7. Open circuit current versus time curves are shown for poled As_2S_3 glass. The sample was poled and depoled at the temperatures indicated on the curves.

the R-C time constant ranges from 4×10^{-3} seconds at 220°C to 4×10^{-1} seconds at 160°C . These results are not in agreement with the data in Figure 7 and Table 1. Additionally, this model will not account for the differences between the open and short circuit curves. A dipolar model and a trapped charge model will also be considered.

By integrating the current vs. time curves over the time we obtain the charge remaining on the sample vs. time for the open and short circuit configurations. These curves are shown in Figures 8 and 9 respectively. The relaxation times for these curves vary considerably. No curve can be described by a single relaxation time. The open and short circuit fast and slow relaxation times are given in Table 2. Again, the fast and slow values are obtained at the beginning and end of each curve respectively. The greatest difference between the open and short circuit polarization curves arise again for the 220°C data. At 200°C the open circuit polarization curve crosses the closed circuit polarization curve from below after approximately eight minutes. The open circuit polarization at 180°C is higher as a function of time than the closed circuit curve; at 160°C it is somewhat lower. This data does not fit the simple dipolar model considered for this glassy system in the following calculations.

DIPOLAR MODEL RESULTS

Consider N_0 dipoles per unit volume of moment p at temperature T in an electric field E . The potential energy of each dipole is

$$U = -\vec{p} \cdot \vec{E} = -pE \cos\theta \quad (4)$$

where θ is the angle between the field and the dipole. The polarization P per unit volume is

$$P = Np \langle \cos\theta \rangle \quad (5)$$

where $\langle \cos\theta \rangle$ is the average over the thermally equilibrated distribution.

From the Boltzmann distribution

$$\langle \cos\theta \rangle = \frac{\int e^{-\beta U} \cos\theta \, d\Omega}{\int e^{-\beta U} \, d\Omega} = \text{ctnh } \beta U - 1/\beta U \quad (6)$$

where $\beta = 1/kT$.

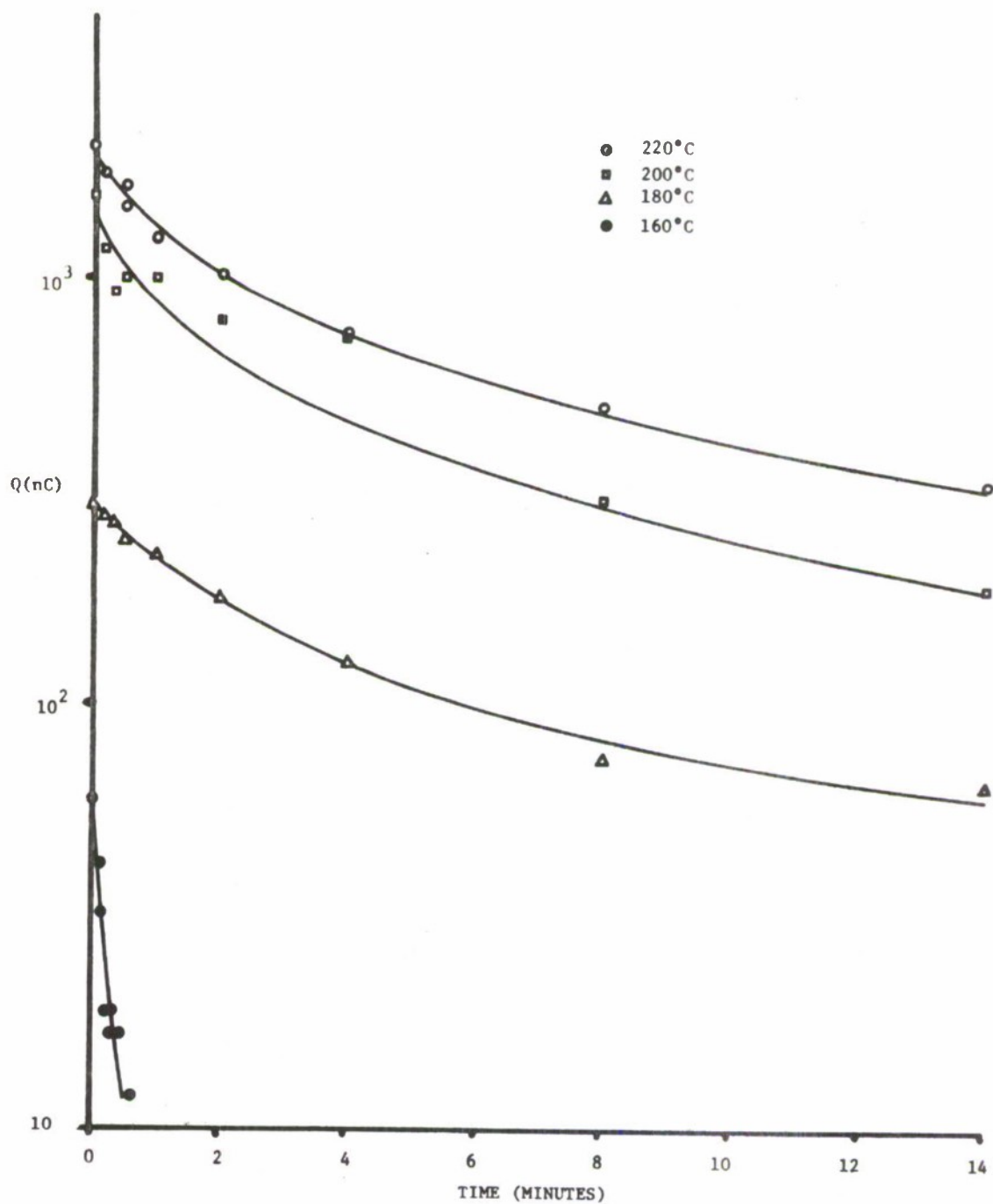


Figure 8. The open circuit polarization versus time curves are shown for As_2S_3 glass after having been poled at the temperatures indicated.

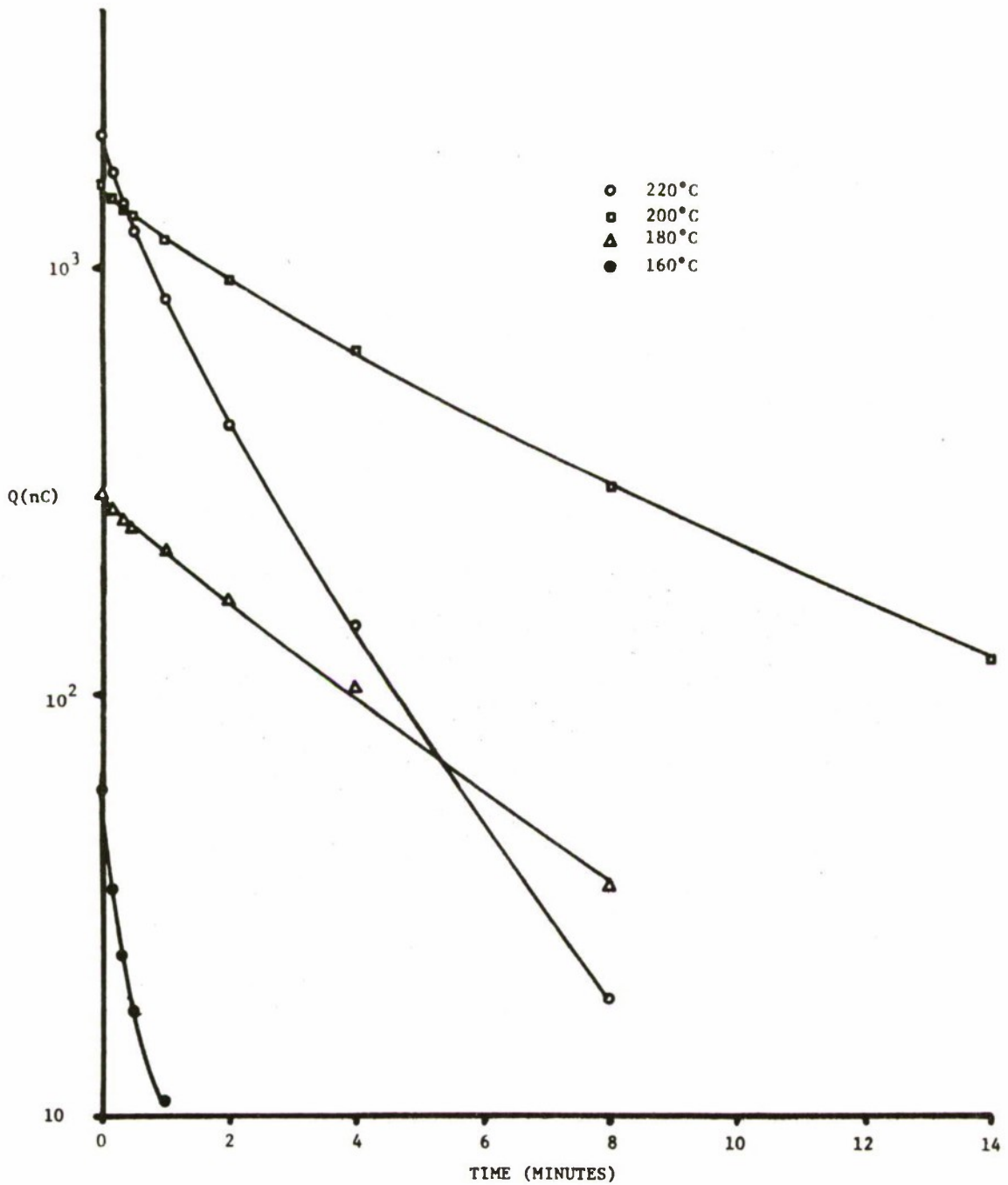


Figure 9. The short circuit polarization versus time curves are shown for As_2S_3 glass after having been poled at the temperatures indicated.

Table 2. The relaxation times for the open circuit and short circuit polarization versus time curves are shown at four temperatures.

TEMPERATURE (°C)	$\tau_{Ch,SC}$ (slow) (seconds)	$\tau_{Ch,SC}$ (fast) (seconds)	$\tau_{Ch,OC}$ (slow) (seconds)	$\tau_{Ch,OC}$ (fast) (seconds)
160	61	18	28	16
180	240	160	920	170
200	380	180	710	136
220	120	50	880	65

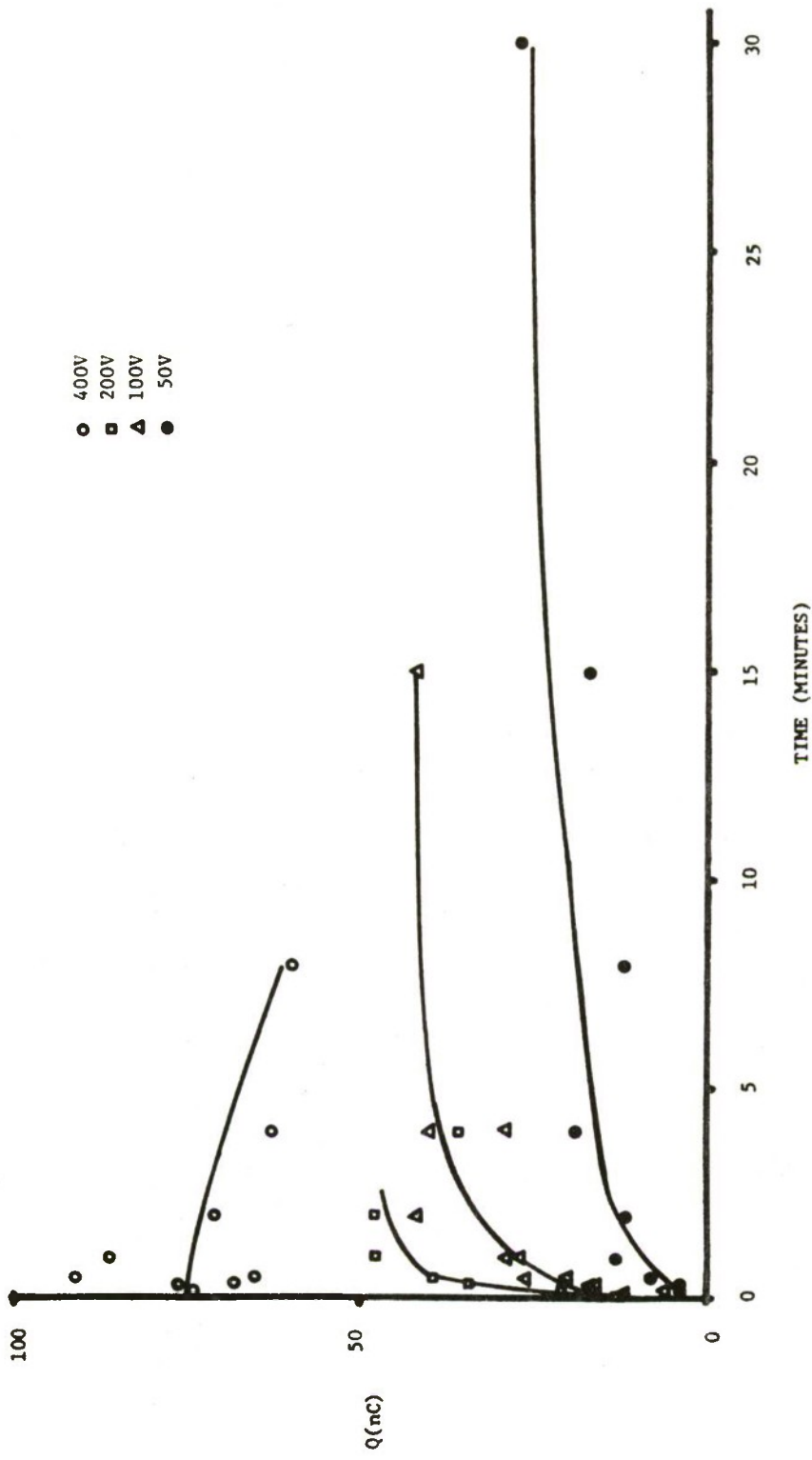


Figure 10. The polarization of As_2S_3 glass is shown as a function of time for various poling voltages at a temperature of 160°C.

For a dipole strength of 10^{-17} esu and a field of 12 kV/cm (40 statV/cm), $pE = 4 \times 10^{-16}$ erg. At room temperature, $kT \approx 4 \times 10^{-14}$ erg. Therefore $pE/kT \sim 10^{-2} \ll 1$ and

$$\text{ctnh } pE/kT - kT/pE \approx pE/3kT \quad (7)$$

$$\therefore P = Np^2 E/3kT \quad (8)$$

For the case of As_2S_3 glass, the probability that an AsS_3 dipole will reorient under the influence of an electric field depends also on how tightly the molecule (dipole) is bound to the neighboring molecules. This means that the number of dipoles available for reorientation depends on the binding energy α and the temperature T . This relationship can be expressed as follows:

$$N = N_0 e^{-\alpha/kT} \quad (9)$$

and therefore

$$P = N_0 e^{-\alpha/kT} p^2 E/3kT \quad (10)$$

As the temperature increases the number of dipoles increases but the disorienting effect of temperature increases as well. There is a peak in the polarization versus temperature curve. By differentiating P with respect to T and setting the function equal to zero one finds the optimum poling temperature

$$T_{\text{opt}} = \alpha/k \quad (11)$$

Two results of this calculation are that the polarization increases linearly with the field; and, the polarization increases with temperature up to T_{opt} and then decreases.

The polarization versus time data for various voltages is shown for temperatures of 160°C, 180°C, 200°C, and 220°C in Figures 10 to 13 respectively. It can be seen from the data that the amount of polarization depends on time, temperature, and field. At any given temperature the amount of polarization saturates with time and with field. This result is not in agreement with Equation (10) in that the polarization does not increase linearly with field. Even under the circumstances where the polarization is increasing with field the increase is not linear. Also, it is highly unlikely that the dipole moment would be large enough to make the approximation in Equation (7) invalid. From Figures 10 to 13 it is evident that the polarization increases markedly with temperature. A plot of the

peak polarization as a function of $1/\text{temperature}$ is shown in Figure 14. However, it is not clear from this curve that there is an optimum poling temperature as is predicted in Equation (11). If an optimum poling temperature exists, it is above 220°C . Additional data above this temperature is difficult to obtain inasmuch as the glass softening point is 195°C .

The fact that the polarization saturates at low voltages would imply that there are a given number of charge traps at a given temperature. These traps are then filled when a voltage is applied to the sample. As was pointed out previously, the charge stored within the sample corresponds to 10^{15} electrons/cm³. This does not correspond to an unusually high trap concentration.

CHARGE TRAPPING⁹

For non degenerate semiconductors, the thermally equilibrated free electron concentration is given by

$$n_0 = N_c \exp \left[(F_0 - E_c)/kT \right] \quad (12)$$

where N_c is the effective density of states in the conduction band, E_c is the lowest conduction band energy, k is the Boltzmann constant, T is the temperature in degrees Kelvin, and F_0 is the equilibrium Fermi energy.

The concentration ($n_{t,0}$) of filled electron traps at energy level E_t is as follows:

$$n_{t,0} = \frac{N_t}{1 + 1/g \exp \left[(E_t - F_0)/kT \right]} = \frac{N_t}{1 + (1/g)(N/n_0)} \quad (13)$$

where $N = N_c \exp \left[(E_t - E_c)/kT \right]$, and

where N_t is the trap concentration and g (degeneracy) is a statistical weighting factor. This is an equilibrium condition which arises from electrons being captured and reemitted into the conduction band. When an electric field is applied to the sample, the balance between the free electron concentration and the trapped electron concentration is changed by the injected charge. In other words, a new equilibrium is found based on the new free electron concentration n . The corresponding quasi-Fermi level F is related to n as follows:

$$n = n_0 + n_i = N_c \exp \left[(F - E_c)/kT \right] \quad (14)$$

⁹M.A. Lampert and P. Mark, "Current Injection in Solids", Academic Press New York (1970).

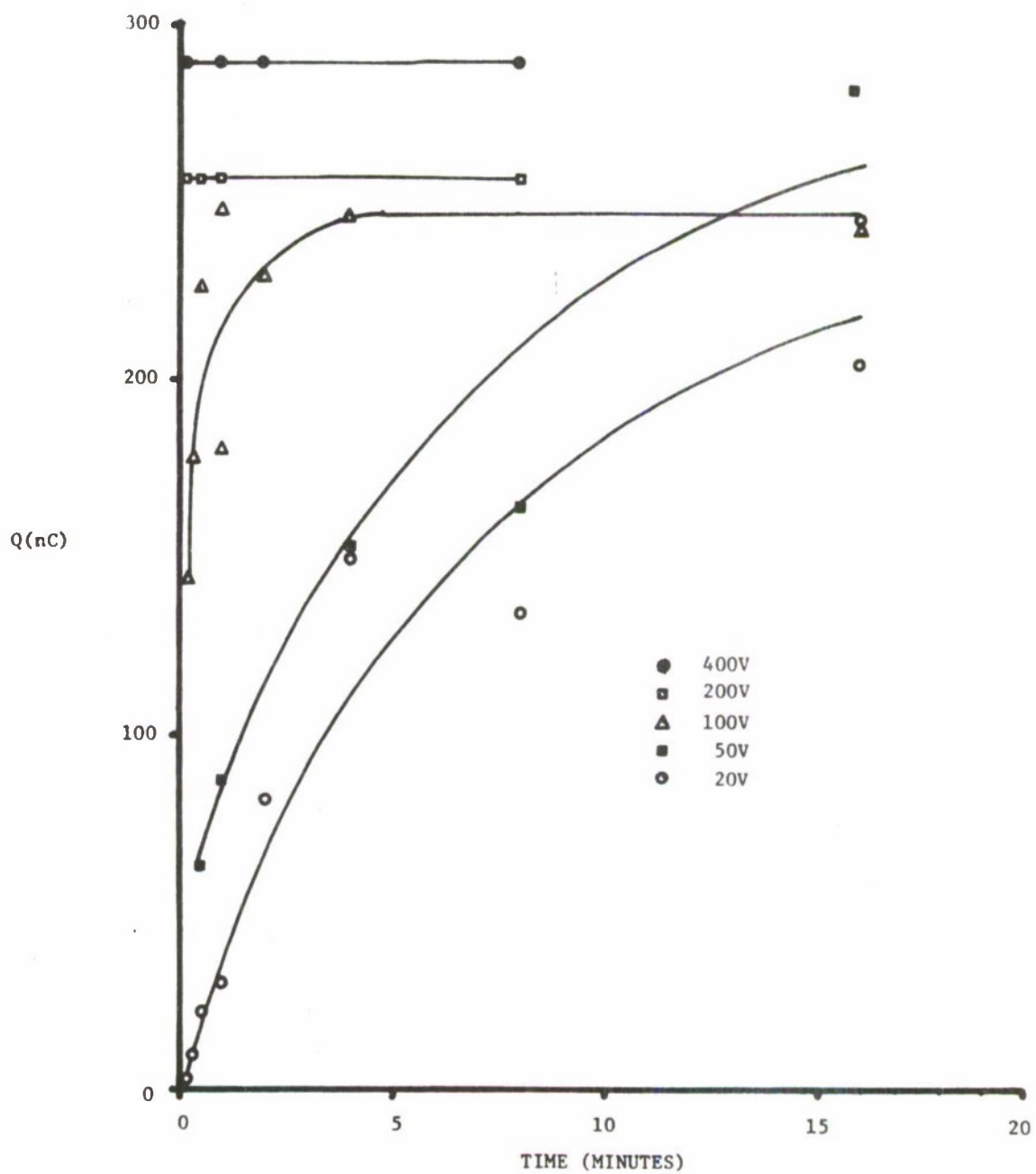


Figure 11. The polarization of As_2S_3 glass is shown as a function of time for various poling voltages at a temperature of $180^\circ C$.

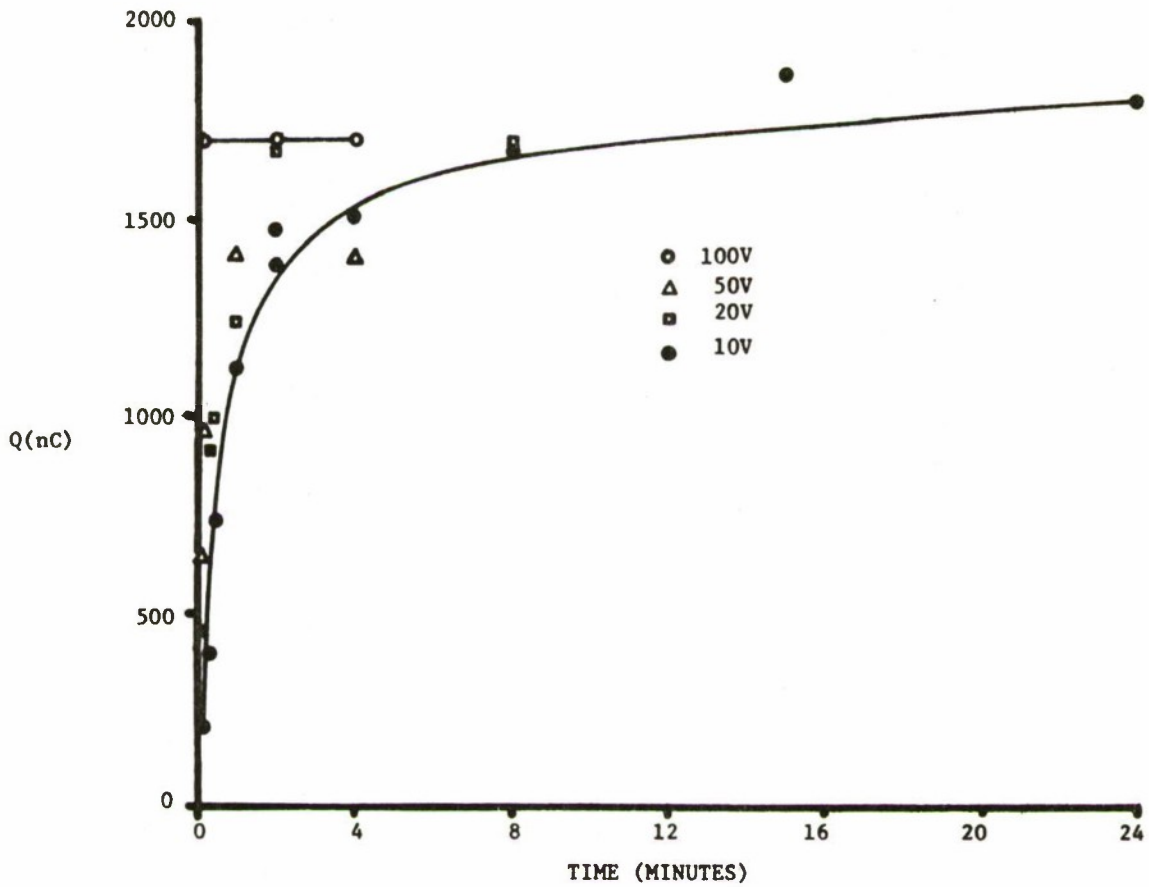


Figure 12. The polarization of As_2S_3 glass is shown as a function of time for various poling voltages at a temperature of $200^\circ C$.

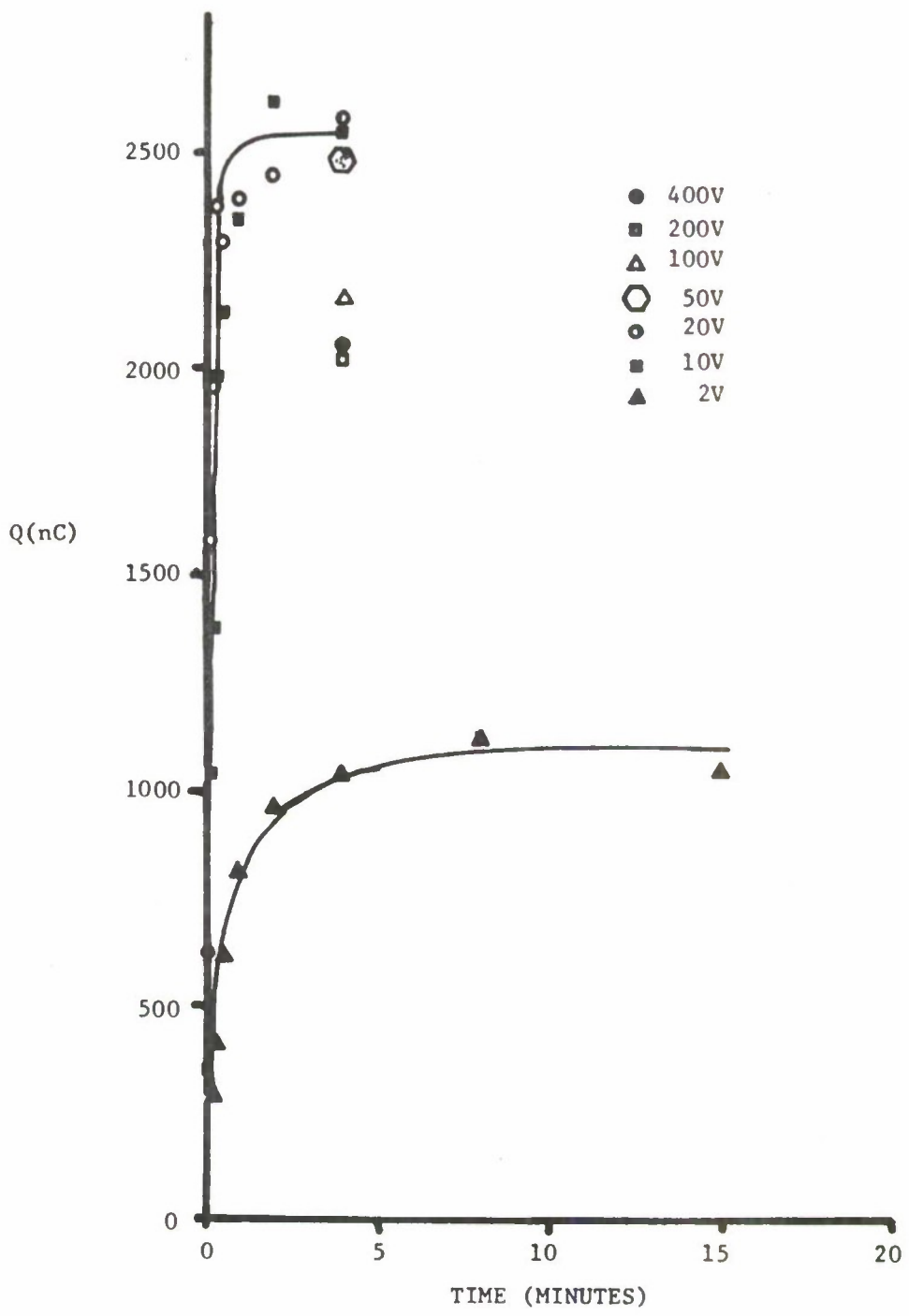


Figure 13. The polarization of As_2S_3 glass is shown as a function of time for various poling voltages at a temperature of $220^{\circ}C$.

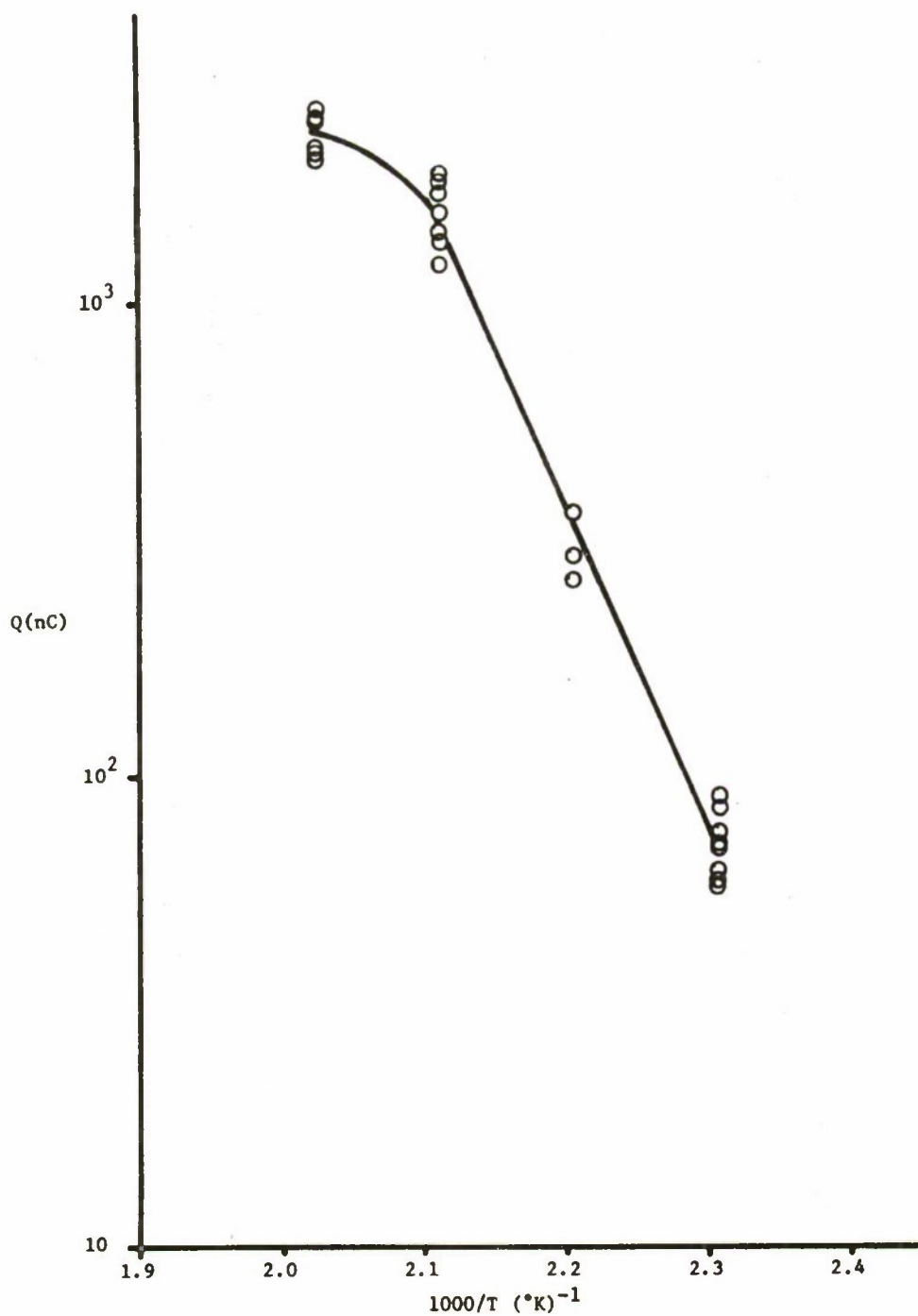


Figure 14. Saturation polarization values are plotted as a function of 1/temperature for As₂S₃ glass.

where n_i is the injected free charge concentration, n_o is the equilibrium free charge concentration, and N_c is the conduction band density of states. Under these circumstances the trapped charge concentration is

$$n_t = n_{t,i} + n_{t,o} = \frac{N_t}{1 + (1/g) \exp [(E_t - F)/kT]} \quad (15)$$

where $n_{t,i}$ is the excess trapped electron concentration due to injection.

The relationship between the free and trapped charges can be obtained by balancing the trapping rate r against the thermal ionization rate g_{th} as follows:

$$r = n \langle v\sigma \rangle (N_t - n_t), \text{ and} \quad (16)$$

$$g_{th} = n_t \langle e \rangle N_c.$$

$$\text{where } r = g_{th} \text{ and } n_t = \frac{N_t}{1 + (\langle e \rangle / \langle v\sigma \rangle) (N_c / n)} \quad (18)$$

In the above equations, v is the magnitude of the free electron velocity, σ is the trap capture cross section, $\langle v\sigma \rangle$ is the average of $v\sigma$ over the free electron velocity distribution, and $\langle e \rangle N_c = \sum_k e_k$, where $\sum_k e_k$ is the probability per unit time of thermal ejection of a trapped electron into conduction band state k summed over all conduction band states.

When the sample is thermally equilibrated, $n = n_o$ and $n_t = n_{t,o}$. By using Equations (13) and (18) we find that

$$\frac{\langle e \rangle_o}{\langle v\sigma \rangle_o} = \frac{N}{gN_c} = \frac{1}{g} \exp \frac{E_t - E_c}{kT} \quad (19)$$

Assuming that R_c and R_e are the electron capture rate and thermal emission rate respectively we have

$$R_c = n/\tau_c, \quad 1/\tau_c = n\langle v\sigma \rangle, \quad (20)$$

$$R_e = n/\tau_e, \quad 1/\tau_e = \langle e \rangle N_e \quad (21)$$

where τ_c and τ_e are the capture and emission lifetimes. Using Equation (19) in Equation (21) we obtain

$$\tau_e = (g/\langle v\sigma \rangle N_c) \exp [(E_c - E_t)/kT]. \quad (22)$$

Evaluating Equation (22) we assume that $g = 1$, $N_c \sim 10^{19} \text{ cm}^{-3}$, $\sigma \sim 10^{-15} \text{ cm}^2$, $\langle v\sigma \rangle \sim 10^{-8} \text{ cm}^3/\text{sec}$, $T = 160^\circ\text{C}$ and 220°C , and therefore, $kT = .037 \text{ eV}$ and $.043 \text{ eV}$ respectively. Equation (22) then becomes $\tau_e \approx 10^{-11} \exp [(E_c - E_t)/kT]$. Values τ_e for various $E_c - E_t$ values are tabulated in Table 3. It is clear from the table that the trap levels that are measured in this experiment are in the range 1.0 to 1.4 eV. The band gap of As_2S_3 is $\sim 2.40 \text{ eV}$. To explore the deeper traps higher temperatures or light of the right wavelength must be employed. The shallower traps have too short a relaxation time to be seen with the experimental techniques employed here. It should also be remembered that a large amount of structural disorder is expected in these samples. This means that the environment can vary substantially from one trap site to the next. Therefore, it is expected that the trap energy will not be well defined. If this is the case, then it is also expected that a variety of relaxation times will be seen. This is exactly the case as is evident in Figure 5 and Table 1.

Another consideration here is the transit time of the electrons across the sample. If this time were slow enough the sample discharge time could be transit time limited. Taking our sample thickness ($d \sim 1/4 \text{ mm}$), the voltage applied ($\sim 400\text{V}$), and a conservative mobility value ($\mu \sim 1 \text{ cm}^2/\text{V sec}$) and using the equation for the transit time ($L^2/V\mu$) we find that the transit time is $\sim 1.6 \times 10^{-6} \text{ sec}$. On the basis of these numbers it can be said that the discharge time of the sample depends on the thermal emission time of the traps.

Applying Equation (15) to the data in Figure 14, it is calculated that $E_t - F \sim 1.3 \text{ eV}$. This means that the dominant trap levels occur at 1.3 eV above the quasi-Fermi level. Assuming small errors in the calculation of the energy levels, the dominant trap levels would occur very close to the conduction band. Traps at this level have too short a lifetime to be measured in these experiments. Also, the fact that the 220°C points do not fit the exponential approximation could be due to the 195°C softening point affecting the trap sites.

CONCLUSIONS

On the basis of this study it is concluded that:

- (a) Aluminum forms a non-diffusing ohmic contact on As_2S_3 .
- (b) Poled As_2S_3 glass stores charge which is released when temperature cycled. The magnitude of the charge depends on temperature and poling voltage.

Table 3. The thermal relaxation times are shown for values of $E_c - E_t$ at temperatures of 160 C° and 220°C.

$(E_c - E_t)$ (eV)	$\tau_e^{220^\circ\text{C}}$ (sec)	$\tau_e^{160^\circ\text{C}}$ (sec)
.1	1.0×10^{-10}	1.5×10^{-10}
.5	1.3×10^{-6}	6.5×10^{-6}
1.0	1.6×10^{-1}	4.2
1.1	1.7	6.1×10^1
1.2	1.8×10^1	8.8×10^2
1.3	1.9×10^2	1.3×10^4
1.4	1.9×10^3	1.9×10^5
1.5	2.0×10^4	2.7×10^6
1.6	2.1×10^5	3.9×10^7
1.7	2.2×10^6	5.7×10^8

(c) The discharge of the samples can be described by a multiple relaxation time process.

(d) The data is not well described by a dipolar model.

(e) The data fits a trapped charge model better than a dipolar model.

(f) The trap levels measured in these experiments are in the range 1.0 to 1.4 eV.

(g) There is no evidence of pyroelectricity in these samples.

REFERENCES

1. R.L. Myuller and Z.U. Borisova, "Solid State Chemistry", Consultant Bureau, New York, pp. 168-179 (1966).
2. F. Kosek and J. Tauc, Czech. J. Phys. B 20, 94 (1970).
3. G. Lucovsky, Phys. Rev. B 6, #4, 1480 (1972).
4. R.J. Kobliska and S.A. Solin, Phys. Rev. B 8, #2, 756 (1973).
5. G. Lucovsky and R.M. Martin, J. Non-Cryst. Solids 8, 185 (1972).
6. D.D. Thornburg, J. Elec. Mat'ls 2, #4, 495 (1973).
7. B.T. Kolomiets, T.F. Mazets, Sh. M. Efendieve, and A.M. Andriesh, J. Non-Cryst. Solids 4, 45 (1970).
8. C. Kittel, "Introduction to Solid State Physics", 3rd Edition, John Wiley & Sons, Inc., New York, p. 307.
9. M.A. Lampert and P. Mark, "Current Injection in Solids", Academic Press, New York (1970).

DISTRIBUTION

Commander
US Army Materiel Command
Alexandria, VA 22333

- 1 Attn: AMCDL,
Mr. N. Klein
- 1 Attn: AMCDL,
Mr. J. Bender
- 1 Attn: AMCRD
- 1 Attn: AMCRD-PT,
Mr. T. Shumacher
- 1 Attn: AMCRD-TP
Mr. P. Chernoff
- 1 Attn: AMCPM-FW,
Mr. R. Cory
- 1 Attn: AMCRD-MT,
Mr. E. Sedlak
- 1 Attn: AMCRD-T,
Mr. R. Zentner
- 1 Attn: AMCRD-PE,
Mr. T. Jasczult
- 1 Attn: AMCRD-G,
LTC M. Ilseman

Commander
US Army Missile Command
Redstone Arsenal, AL 35809

- 1 Attn: AMSMI-RR,
Dr. G. Miller
- 1 Attn: AMSMI-RR,
LT. J. Hammond
- 1 Attn: AMSMI-R,
Dr. J. McDaniel
- 1 Attn: AMSMI-REI,
Mr. John Asbell

Commander
Aberdeen Proving Ground
Aberdeen, MD 21005

- 1 Attn: AMSTE-SA-E,
Mr. J. Bialo
- 1 Attn: STEAP-DS-TF
- 1 Attn: AMXHE-SYS,
Mr. G. Horley
- 1 Attn: AMXBR-TD,
Dr. R. Eichelberger
- 1 Attn: AMXSY-GS,
Mr. C. Odom
- 1 Attn: AMXSY-D,
Dr. J. Sperrazza

Commander
US Army Armament Command
Rock Island, IL 61201

- 1 Attn: AMSAR,
MG J. Raaen
- 1 Attn: AMSAR-RDT,
Mr. J. Turkeltaub
- 1 Attn: AMSAR-RDT,
Mr. W. Beyth
- 1 Attn: AMSAR-RD,
Mr. J. Brinkman
- 1 Attn: AMSAR-RDE,
Mr. E. Vaughan
- 1 Attn: AMSAR-RDT,
Dr. R. L. Moore
- 1 Attn: AMSAR-RD,
COL L. Sherman

DISTRIBUTION (Cont'd)

Commander
US Army Dugway Proving Ground
Attn: STEDP-TL, Technical Library
Dugway, UT 84022

Commander
White Sands Missile Range
White Sands, NM 88002

1 Attn: AMSEL-W-MJ,
LTC R. Coon

1 Attn: AMSEL-WL-ML,
Mr. J. Bert

1 Attn: STEWS-ID-A,
Mr. G. Galos

Commander
US Army Electronic Proving Ground
Attn: STEEP-T-B1
Ft. Huachuca, AZ 85613

Commander
Yuma Proving Ground
Attn: STEYP-AD, Technical Library
Yuma, AZ 85364

Commander
US Army Tropic Test Center
Attn: STETC-MO
APO, New York 09827

Commander
US Army Field Artillery School
Ft. Sill, OK 73503

1 Attn: Director of Combat &
Training Developments

1 Attn: Doctrine Division

1 Attn: Artillery Support Division

1 Attn: Studies Division

Commander
US Army Tank Automotive Command
Attn: AMSTA-Z, Mr. R. McGregor
Warren, MI 48090

Commander
Combat Systems Group (CACDA)
Ft. Leavenworth, KS 66027

1 Attn: Terminal Homing Task Force,
COL DeShazo

1 Attn: Technical Director,
Dr. L. Follis

1 Attn: LTC J. Gower

Commander
Training & Doctrine Command
Ft. Belvoir, VA 22060

1 Attn: ATCD-CS-F,
LTC Davis

1 Attn: ATCD-CS-I,
LTC Griminger

Commander
USACDC, Infantry Agency
Ft. Benning, GA 31905

1 Attn: CDCINA-S,
MAJ Gibbs

1 Attn: CDCINA-S,
MAJ Binkewicz

1 Attn: CDCINA-CM,
MAJ McDonald

Commander
Edgewood Arsenal
Attn: SAREA-DE-MM, Mr. D. Anderson
Aberdeen Proving Ground, MD 21010

Commander
US Army Materials & Mechanics
Research Center
Attn: AMXMR-D. Mr. R. Fitzpatrick
Watertown, MA 02172

DISTRIBUTION (Cont'd)

Commander
Harry Diamond Laboratories
2800 Powder Mill Road
Adelphia, MD 20783

1 Attn: AMXDO-TIB

1 Attn: AMXDO-RCB,
Mr. H. Gibson

1 Attn: AMXDO-RCB,
Dr. T. Gleason

Commander
US Army Research Office-Durham
Box CM, Duke Station
Attn: Dr. R. J. Lontz
Durham, NC 27706

Commanding General
US Army Natick Laboratories
Attn: AMXRE-PRD, Dr. E. Healy
Natick, MA 07162

Commander
US Army Electronics Command
Night Vision Laboratory
Attn: AMSEL-NV-VL, Mr. W. Lyttle
Ft. Belvoir, VA 22060

Commander
Naval Missile Center
Pt. Mugu, CA 93042

1 Attn: Mr. J. Kearney

1 Attn: Mr. Mark, Code 5351

1 Attn: Mr. Stephenson, Code 5351

Commander
Naval Research Laboratory
Washington, DC 20390

1 Attn: Dr. Anderson, Code 6550

1 Attn: Dr. A. Schindler, Code 6330

Commander
Wright-Patterson AF Base
Attn: AFAL/WRW, Mr. A. R. Torres
Dayton, OH 45433

Commander
Air Force Armament Laboratories
Attn: DLOS
Elgin AFB, FL 32542

Commander
USASA/ODCSRND
Arlington Hall Station
Attn: Mr. Abercrombie
Arlington, VA 22212

Commander
US Army Combat Developments Experi-
mentation Command
Ft. Ord, CA 93941

1 Attn: CDCEC-PPA-PA,
CPT Macia

1 Attn: CDCEC-EX-E,
Project Officer

1 Attn: CECEC-EX-E,
MAJ F. Isgrig

Commander
US Army Armament Command
Attn: AMCPM-CAWS, COL Post
Rock Island Arsenal, IL 61201

Commander
Ft. Hood
Attn: MASSTER, MAJ Alexander
Killeen, TX 76544

Commander
US Army Electronics Command
Ft. Monmouth, NJ 07703

1 Attn: AMSEL-KL-DT,
Mr. B. Louis

1 Attn: AMSEL-CT-L,
Dr. R. Buser

1 Attn: AMSEL-CT-L,
Mr. V. DeMonte

1 Attn: AMSEL-CT-L,
Mr. M. Mirachi

DISTRIBUTION (Cont'd)

US Army Foreign Science &
Technology Center
Attn: AMXST-BS (Stop 196)
Munitions Bldg.
Washington, DC 20315

President
US Army Armor & Engineering Board
Attn: STEBB-CV
Ft. Knox, KY 40121

Atmospheric Science Laboratory
USAECOM
White Sands Missile Range,

1 Attn: SELWS-E,
Mr. M. Diamond

1 Attn: AMSEL-BL-MS,
Mr. R. B. Gomez

Director Electronic Warfare
Electronic Warfare Laboratory
Ft. Monmouth, NJ 07703

1 Attn: AMSEL-WL-D,
Mr. J. Charlton

1 Attn: AMSEL-WL-D,
Mr. C. Hardin

Department of the Air Force
Air Force Avionics Laboratory
(AFSC)
Wright-Patterson AFB, PH 45433

1 Attn: Mr. R. Firsdon

1 Attn: ASD/RWT

Air Force Weapons Laboratory
Kirtland Air Force Base
Attn: CPT M. Kemp, Bldg. 497
Albuquerque, NM 87116

Director
Eustis Directorate
US Army Air Mobility R&D
Laboratory
Attn: SAVDL-EU-SS, Mr. J. Ladd
Ft. Eustis, VA 23604

US Army Research Office
Room 1A881, Pentagon
Washington, DC 20301

1 Attn: DARD-ARS-PP,
MAJ A. Mullin

1 Attn: DARD-ARS-PP,
Dr. J. I. Bryant

1 Attn: DARD-ARS-PP,
Dr. R. Watson

Office of the Deputy Assistant
Commander for Combat Developments
and Training
Ft. Knox, KY 40121

1 Attn: ATSAR-CD-S,
COL Davis

1 Attn: ATSAR-CD-M,
COL Bradley

Advisory Group on Electron Devices
Attn: Secretary Working Group on
Lasers
201 Varick Street
New York, NY 10014

Mr. Douglas Beatty
ODDR&E, Air Warfare
Pentagon
Room 3E1047
Washington, DC 20301

LTC Robert D. Resley
HQDA (DARD-ART)
Pentagon
Room 3D358
Washington, DC 20301

LTC B. Krawetz
Office of Ass't Secty Defense
Intelligence Office
Pentagon, Room 3C200
Washington, DC 20301

DISTRIBUTION (Cont'd)

LTC F. Palermo
 Pentagon
 Attn: DARD-DD-M-F,
 Room 3C367
 Washington, DC 20301

Dr. R. E. Schwartz
 Pentagon
 Attn: ODDR&E/TWP, Rm. 3E1025
 (Land Warfare)
 Washington, DC 20301

Dr. John Porter
 Pentagon, ODDR&E/EW&R
 Room 3D139
 Washington, DC 20301

LTC Guest
 HQ, USAF
 Pentagon
 Attn: AF/RDP, Room 4D274
 Washington, DC 20301

COL Richard McLean
 Weapons System Evaluation Group
 400 Army/Navy Drive
 Arlington, VA 22202

Mr. F. Reed
 Product Manager
 Aircraft Survivability Equipment
 P.O. Box 209
 St. Louis, MO 63166

MG S. Meyer
 Commander
 Attn: MASSTER
 Ft. Hood, TX 76544

Mr. Everett Richey
 School of Aerospace Medicine
 Brooks Air Force Base
 San Antonio, TX 78235

Dr. M. P. Pastel
 Scientific Advisor-TRADOC
 Attn: ATDC-SI
 Ft. Monroe, VA 23651

Advanced Research Projects Agency
 Architect Bldg.
 1400 Wilson Blvd.
 Arlington, VA 22209

1 Attn: Dr. E. Gerry

1 Attn: Dr. P. Clark

Assistant Director
 Engineering Technology
 Pentagon

Attn: ODDR&E, Room 3E1060
 Mr. J. Persch
 Washington, DC 20301

Defense Documentation Center (2)
 Cameron Station
 Alexandria, VA 22314

Frankford Arsenal:

1 Attn: AOA-M/107-B

1 Attn: TD/107-1

1 Attn: PD/64-4

1 Attn: PDR/64-4

1 Attn: PDS/64-3

4 Attn: PDC/64-3

1 Attn: FC/110-1

1 Attn: FCD-O/201-2
 Mr. S. C. Novak

1 Attn: FI/107-B

1 Attn: PA/107-2

1 Attn: QA/235-3

3 Attn: TSP-L/51-2
 1 - Reference Copy
 1 - Circulation Copy
 1 - Tech Rpts Editing

Printing & Reproduction Division
 FRANKFORD ARSENAL

Date Printed: 10 February 1976